

HEALTH EXAMINATION BASED ON IRIS IMAGES

CHENG-LIANG LAI , CHIEN-LUN CHIU

Department of Informatics, Fo Guang University, R.O.C.
E-MAIL: Lai630630@gmail.com

Abstract:

This study combined iridology with image processing technique to conduct iris disease examination. Iridology is not to determine disease, but to reflect degeneration of organic functions, toxin precipitation and various unhealthy situations caused by mental or other factors. Iris test technique applies simple and non-invasive healthy examination method, helps the people prevent disease, and regularly follows up self-health conditions to achieve real-time prevention and treatment.

The system consists of four modules: eye image capture, image preprocessing, texture feature extraction and symptomatic analysis. Following the input of eye image, the required iris part is acquired from eye images by using image preprocessing module. The texture feature extraction module utilizes 2-D Gabor filter to extract texture feature. The symptomatic analysis module uses fuzzy theory to evaluate severity of organ symptoms.

Keywords:

Iridology; 2-D Gabor filter; Fuzzy theory;

1. Introduction

Iridology has a history of over 3000 years, and has long been used to examine disease in Tibet and India. Iridology was proposed in the 1800s by Dr. Ignatz Von Peczely, who found a black line in the eyes of an injured owl. He continued to observe the owl after it recovered, and found curved white line appeared at the position where original black line existed. The black line later became a black point, and surrounded by white shade. During his undergraduate study, he had the chance to observe iris of injured patients who received surgery, and explored their iris changes, which were related to their injuries, operations or disease. Dr. Peczely devoted to the study of changes of eyeballs and iris when people are ill, and plotted the first iris map.

Similarly, a clergyman also found the unique relationship between the change of color in eyes and hyper pigmentations. Since the 19th century, iridology has developed rapidly, and many scientists and doctors studied iris, and corrected and improved the iris map. Bernard Jensen, an American doctor and the vanguard of iris study, conducted

clinical experiments for over 50 years to develop detailed left and right iris reflex zone map [1]. Nils Liljequist, a Swedish missionary, found that the changes of eyes are related to hyper pigmentations. Since then, iridology has developed prosperously. In Taiwan, iris was developed in 1988 after Dr. Chung of Veterans General Hospital published the Chinese version of “*Science and Practice of Iridology*” written by American iridologist Dr. Beruward Jensen. From then on, many researchers have devoted to iris research. At present, iridology is widely used in natural therapy, preventive medicine, clinical diagnosis and mental therapy.

Features of iris: Iris is an extension of brain, and there are ten thousands of neural microvascular, muscle fibers and other tissues. Their characteristic patterns and their spatial relation should be analyzed and quantified for recognition.

Singularity of iris: Iris is unique because of its complicated form, and its complex surface structure is due to its patterns depending on embryonic gene. Iris has limitation in genetic expression (not only pattern, function, coloration and apparent texture). Even the irises of identical twins are very different, which can be distinguished. Therefore, even with the same genome, each person has their own unique iris, just like fingerprints. According to statistics, the probability of the two identical irises is 1 in 10^{78} .

Stability of iris: Although iris is weak, it is still covered by eyelid and cornea (see Figure 1) and often protected by glasses or contact lenses. In addition, iris is not easily polluted. Naturally, people think iris and eyes are the most protected organs. Features of iris remain the same from 1 year old to death, if not considering degeneration or disease.

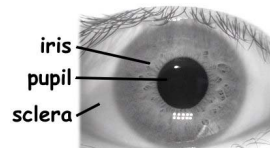


Figure 1. Eye iris image.

In the Western medicine, iris is connected to ten thousands of nerve fibers, blood capillaries, muscles and other tissues through brain, and it reflects relevant organs so

as to test deterioration of organs. Health of body organs can be analyzed through holes, fracture, flecks, lines and color of iris.

In Oriental medicine, Chinese medicine applies ophthalmic diagnosis, i.e. five wheels and eight belts. Five wheels: eyelid is flesh wheel, belonging to spleen; canthus is blood wheel, belonging to liver; black of eye is wind wheel, belonging to lung; pupil is water wheel, belonging to kidney. Clearly, eyes are external mirror of viscera and can reflect health of viscera. Five wheels belong to the relation between five-zang viscera, and health of viscera can be observed by five wheels to judge pathological changes of the relevant viscera, and to know body disease information as early as possible. Eyes are closely related to six-fu viscera gallbladder, stomach, large intestine, sanjiao, urinary bladder. Six-fu viscera can absorb and digest some nutriments to nourish eyes. Zang viscera are closely linked to fu viscera in pathology. Zang viscera disease can transmit to fu viscera, vice versa. Thus Zang viscera and fu viscera should be studied if abnormality of eyes occurs. By combining Western medicine with Oriental medicine, and using spinal cord system for disease examination, more accurate results can be achieved.

From 1996 to 1997, Russian government supported iris images of 800,000 patients for iris studies conducted by the Korean government. The experimental data include:

- 90.2% accuracy for digestive system
- 86.4% accuracy for endocrine system
- 72.2% accuracy for musculo-skeletal system
- 79.7% accuracy for nervous system
- 85.7% accuracy for uro-genital system
- 81.6% accuracy for circulatory system
- 54.2% accuracy for immune system

2. Research methods

Iridiagnosis system framework consists of four modules: human's eye image capture, image preprocessing, texture feature extraction and symptomatic analysis. The first step is eye image capture, taking eye image and acquiring information. The second step is to process the eye images and acquire iris information; the third step is texture feature extraction, in which 2-D Gabor filter is used to detect texture direction and obtain eigenvalue; the last step is symptomatic analysis, displaying sign of disease through fuzzy theory after statistics of eigenvalues.

This study first reviews discussion and analysis of texture feature extraction in the past studies. In 1993, John Daugman [2] [3] proposed an excellent iris recognition system. This system uses standard video capture device to take eye image out of a distance of 30 cm, and acquire iris

image following analysis of human eye image. Phase information of the complex number generated from 2-D Gabor filter is selected, and real and imaginary parts are quantified into 1 bit, totaling to 256 bytes in iris code. Hamming distance is used to identify similarity. Wildes et al. [4] used Laplacian Pyramid to compile iris code in 1996, and designed another iris recognition system. The system uses Laplacian Pyramid to decompose iris images and selects four different band-pass images as iris samples. There is an inevitable problem for iris recognition: move, zoom in and out, turn the images, correct the relevant equations and calculate correlation for contrast and recognition. However, compared to Daugman, using binary code and Hamming distance shows good speed; Wildes system speed is affected by calculation.

Adhi Dharma Wibawa and Mauridhi Hery Purnomo[5] suggested real-time iris images to examine pancreatic gland of diabetic patients in 2006. Among the 34 patients who were examined through tissue cell homogenizer, the accuracy rate reached 94%, and among the 6 patients who received pancreatic gland examination, the accuracy rate was 100%.

In 2007, Lin Ma and Naimin Li [6] suggested that texture feature and classification could be used for iridiagnosis. Experts removed bright spots in iris by using self-adaptability adjacent insertion approach and applied standard round to fast pupil location based horizontal and vertical grey-level images. 2-D Gabor filter was used to analyze texture and estimate its fractal dimension for extraction of pathological characteristics, and Support Vector Machines (SVM) was utilized to examine disease of digestive tract and neurological disease. Among the 429 patients examined, the accuracy rate was 86.4% for neurological disease and 84.9% for disease of digestive tract. These mean iris model is very effective and can be used for medical diagnosis or public application.

R.A.Ramlee and S.Ranjit [7] suggested iris recognition for cholesterol examination in 2009. The results showed that the incidence of cholesterol was high when eigenvalue exceeded a threshold value.

Fuzzy theory [8], proposed by Zadeh, can be applied to semantic ambiguity, especially the fuzzy components in semantics. Fuzzyness described by fuzzy theory is uncertainty of degree and express probability. Fuzzy theory achieves better results in artificial intelligence, control and image recognition.

Fuzzy theory has been used in image segmentation in recent years, and similar sections form image for cluster [9]. Andrei Doncescu suggested a cluster approach that can segment noisy images and automatically adjust membership function and cluster number.

Isak Gath suggested a new approach to detect elliptical or ring images for clustering [10]. The approach is to obtain

the best ellipse and deduce two focal points and two diameters based on elliptic equation. Fuzzy k-Ellipses (FKE) is used to calculate data synchronously and find multiple crossing ellipse, concentric ellipse, incomplete ellipse and hidden line of them.

Fuzzy theory analysis can be divided into:

1. The input values include two parts, and the first is distribution ratio of characteristic points in image. The feature image is 50*28 pixels, in which each white point is a characteristic point, and then all characteristic points are accumulated for distribution proportion of characteristic points which act as fuzzy set of X . The fuzzy set of X is divided to X_{small} , X_{medium} and X_{big} .
The greater proportion is, the bigger holes of iris.
2. The characteristic points of feature image have different sections, and namely white pixel is not formed by single point. A large cluster consists of many multipoint white pixels. The clusters are separated by connected components for image processing, forming fuzzy set of Y in terms of cluster number. However fuzzy set of Y can be classified into Y_{few} , Y_{medium} and Y_{many} according to cluster number. The more cluster number is, the more holes of iris are.
3. The final result is divided into three fuzzy sets of Z , which is used to display severity of symptoms, Z_{weak} , Z_{medium} and Z_{strong} .

From the past experience for creation of fuzzy rule base, X set denotes the distribution ratio of characteristic points, Y set denotes the cluster number, and Z set denotes the feature intensity. Table 1 shows the creation of fuzzy rule base. As seen, the distribution of iris characteristic points is closely related to severity of symptoms.

TABLE 1 CREATION OF FUZZY RULE BASE.

| | |
|--------|--|
| Rule 1 | If X_{small} and Y_{few} then Z_{weak} |
| Rule 2 | If X_{medium} and Y_{few} then Z_{weak} |
| Rule 3 | If X_{big} and Y_{few} then Z_{medium} |
| Rule 4 | If X_{small} and Y_{medium} then Z_{medium} |
| Rule 5 | If X_{medium} and Y_{medium} then Z_{strong} |
| Rule 6 | If X_{big} and Y_{medium} then Z_{strong} |
| Rule 7 | If X_{small} and Y_{many} then Z_{strong} |
| Rule 8 | If X_{medium} and Y_{many} then Z_{strong} |
| Rule 9 | If X_{big} and Y_{many} then Z_{strong} |

Symptoms are displayed through severity after fuzzy

theory analysis, so the examined patients can know whether they have disease and their health conditions.

3. Experimental process

The system framework consists of eye image capture, image preprocessing, texture feature extraction and symptomatic analysis. The detailed process is shown in Figure 2.

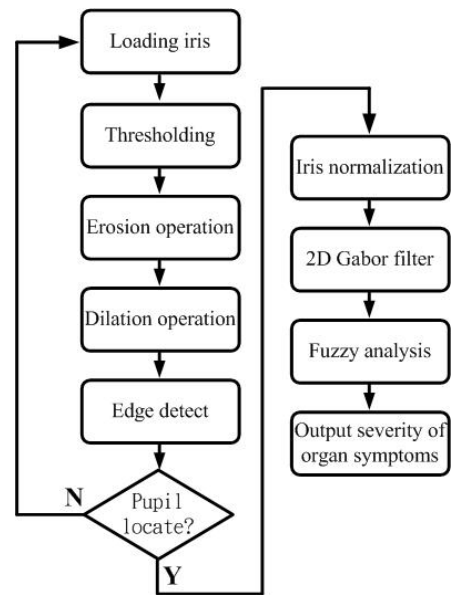


Figure 2. System flow chart.

3.1. Thresholding

There are many approaches for pupil location [11] [12], and extremely deep pupil color means extremely low grey level. Thus, this paper uses threshold value to separate pupils and other parts (iris and sclera). Thresholding is one of the important approaches of image segmentation. The obvious approach of extracting a pixel from background is to select a threshold value to separate the two models. For (x, y) , if $f(x, y) > T$, it is called background point, otherwise, object point. Binarization image $g(x, y)$ is defined as follows:

$$g(x, y) = \begin{cases} 0 & f(x, y) > T \\ 1 & f(x, y) \leq T \end{cases} \quad (1)$$

3.2. Opening

This study uses erosion and dilation in morphological operations to eliminate noise [2]. The morphological operations refer to the study of the form or shape of an

organism and equipment; if it is applied to image processing, it can simplify object shape and act as noise filter. Another application is to strengthen object structure, such as thinning, thickening, and convex hull. The approaches often used to eliminate background noise and reinforce image structure are as follows:

(I) Erosion: contract an object into several pixels inward. Erosion equation is as follows:

$$X \ominus H = \{(x, y) : H_{(x,y)} \cap X \neq \emptyset\} \quad (2)$$

(II) Dilation: dilate an object into several pixels outward. Dilation equation is as follows:

$$X \otimes H = \{(x, y) : H_{(x,y)} \subseteq X\} \quad (3)$$

(III) Opening: dilation is performed after erosion. The objective is to remove unnecessary points or lines and recover image and eliminate noise outside the object after dilation operation. The opening equation is as follows:

$$X \circ H = (X \otimes H) \ominus H \quad (4)$$

(IV) Closing: erosion is performed after dilation. The objective is to fill the inner small holes and gaps, and fill back and collect broken lines. The closing equation is as follows:

$$X \bullet H = (X \ominus H) \otimes H \quad (5)$$

To eliminate noise caused by eyelash, this paper uses 10 x 10 matrix to conduct erosion operation for eliminating noise. Then the same matrix can be used for dilation operation to recover eroded periphery of pupils, i.e. opening.

3.3. Edge detection

After pupils are cut successfully, and central point can be found. First, edge points are detected to calculate average value through summation of coordinates and to get central point of pupil. The method is partial to center of mass, and the difference is in many cases the pupils are not always round. Therefore, that equation of a complete circle uses center and radius to define pupils is biased. Furthermore, from another viewpoint, if the pupil is totally round, calculation of center of mass is still feasible.

Edge detection is often used to separate objects, and so far it is the common method to detect meaningful discontinuity. In the course of edge detection, this paper employs Sobel for edge detection because Sobel [13] can provide differential value and features smoothing effect. The following equation represents shield of G_x and G_y of horizontal and vertical vector gradient. The operation of shield around the image is finished by using adjacent points.

$$\underline{G}_x = \begin{Bmatrix} -1 & -2 & -1 \\ 0 & 0 & 0 \\ 1 & 2 & 1 \end{Bmatrix} \quad \underline{G}_y = \begin{Bmatrix} -1 & 0 & 1 \\ -2 & 0 & 2 \\ -1 & 0 & 1 \end{Bmatrix} \quad (6)$$

After using two different Sobel edge detection gradient (horizontal and vertical operation) operations, this paper gathers detected points to calculate edge points of all pupils and extract coordinates of them.

3.4. Pupil location

After the edge points of all pupils are calculated, and thus pupil center can be determined by aggregating and averaging the edge points.

3.5. Iris normalization

This paper utilizes Rubber Sheet Model suggested by Daugman [3] for easy treatment of subsequent feature extraction module. Ring-shaped image of iris is normalized into a rectangular image after conversion of polar coordinate and Cartesian coordinate, as shown in Figure 3. Due to iris is affected by pupils, like system hypothesis, scaling can be regarded as nonlinear changes. In process of polar coordinate conversion, linear interpolation is used for normalization of iris texture scaling.

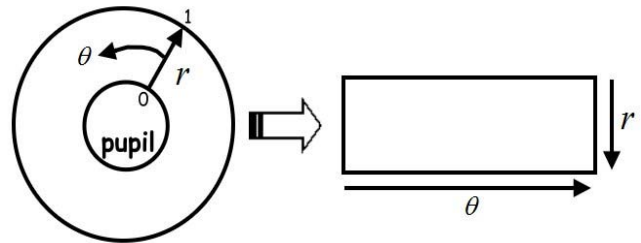


Figure 3. Daugman's rubber sheet model.

From Cartesian coordinate to non-coaxial center, and iris image $I(x, y)$ is redefined, and equation is as follows:

$$I(x(r, \theta), y(r, \theta)) \rightarrow I(r, \theta) \quad (7)$$

where

$$x(r, \theta) = (1-r)x_p(\theta) + rx_l(\theta) \quad (8)$$

$$y(r, \theta) = (1-r)y_p(\theta) + ry_l(\theta) \quad (9)$$

$I(x, y)$ is defined as iris region image, (x, y) is Cartesian coordinate, (r, θ) is normalized polar coordinate, and furthermore x_p, y_p and x_l, y_l is the pupil coordinate and direction where iris is along θ .

Daugman [2] used radial dilation for compensation, and pupils to change a simple model of linear enhancement. The pupils are unable to correspond to iris, so angles between outer ring of iris and pupils must be recalculated. The equation is presented as follows:

$$r' = \sqrt{\alpha\beta \pm \sqrt{\alpha\beta^2 - \alpha - r_l^2}} \quad (10)$$

where

$$\alpha = o_x^2 + o_y^2 \quad (11)$$

$$\beta = \cos\left(\pi - \arctan\left(\frac{o_y}{o_x}\right) - \theta\right) \quad (12)$$

o_x and o_y denote the corresponding iris center while pupil center rotates, and r_l is defined as iris radius.

3.6. Feature extraction of 2-D Gabor iris

In recent years, Gabor filter is widely used in image process field, and further image texture has highly efficient performance speed. In the spatial region, a 2-D Gabor filter [11] can be expressed by the following equation:

$$\begin{cases} g(x,y) = g'(x,y)\exp(j2\pi\omega\xi) \\ g'(x,y) = \frac{1}{2\pi\sigma^2} \exp\left(-\frac{x^2+y^2}{2\sigma^2}\right) \\ \xi = x\cos\theta + y\sin\theta \end{cases} \quad (13)$$

(x,y) is the coordinates of spatial region, σ is the Gauss standard deviation function, and ω the is frequency component and θ is the direction of filter parameters.

3.7. Fuzzy analysis

In the last analysis step, this paper applies fuzzy theory for analysis of severity of symptoms, and thus the first input value is proportion of characteristic points and holes number. Fuzzy set of X denotes the proportion, and fuzzy set of Y denotes hole number. Fuzzy set of X varies from 0 to 1, but fuzzy set of Y is hole number, i.e. cluster number, ranging from 0~15. The final result of Z set describes severity of symptoms, from 0~1 %. X set has three Gaussian fuzzy functions (0, 0.2353, 1) and variables are 0.1, 0.1 and 0.4, as shown in Figure 4. Y set has three Gaussian fuzzy functions (0, 4, 15), variables are (2, 2, 6), as shown in Figure 5. Z is shown in Figure 6.

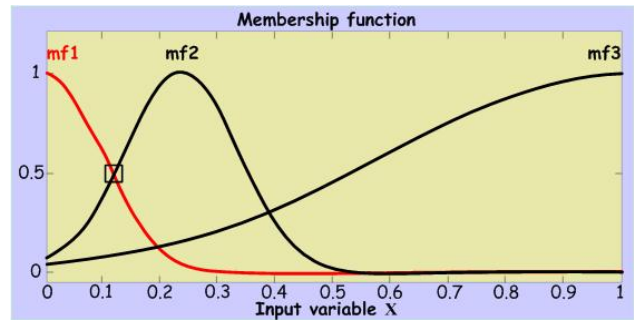


Figure 4. Distribution relation of X set.

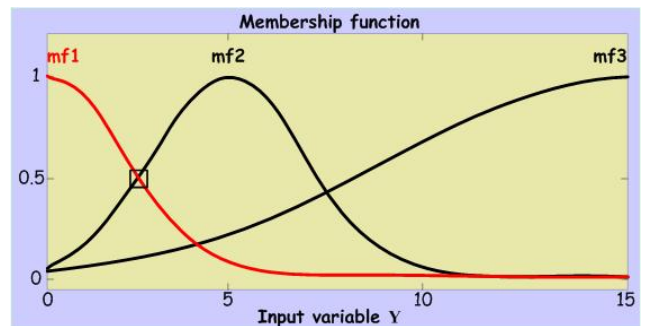


Figure 5. Range of cluster number of Y set.

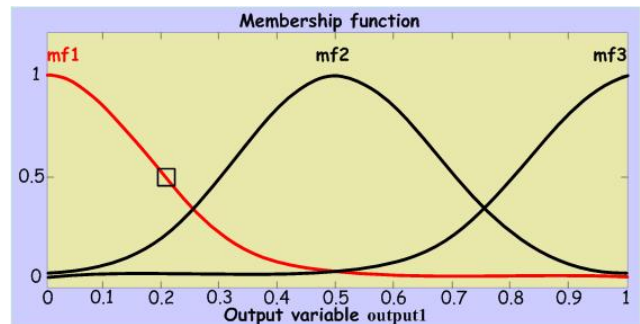


Figure 6. Severity of symptoms of Z set.

4. Experimental Results

This study totally collected 75 iris images, but after feature extraction 64 iris images can be used. The resting 11 images cannot be used due to environment factors, including:

- Bright spot falls on lung due to shooting light source. See Figure 7.
- Covered by eyelids (eyelash is included).
- In the shooting place not suitable for eyes.
- Light source cannot make pupils contract. See Figure 8.

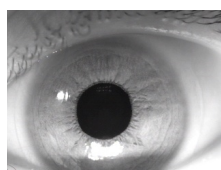


Figure 7. Bright spot falls on lung area.

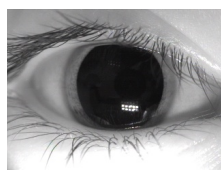


Figure 8. Light source cannot make pupils contract.

Among the 64 iris images, 41 images are the irises of persons who often smoke or live in polluted environment, and other 23 images are shot from healthy irises.

The experimental results indicate image processing technique including thresholding, morphological operation, edge detection, iris normalization, 2-D Gabor filter, fuzzy theory can be used to reflect severity of organ disease.

TABLE 2 EXPERIMENTAL RESULTS. COVERAGE OF SYMPTOMS IS DOWN TO 20%.

| Quantity | Cluster number | Symptom coverage (%) | Severity of symptoms |
|----------|----------------|----------------------|----------------------|
| 51 | 0~4 | 0~19 | 0.177290~0.459997 |

TABLE 3 EXPERIMENTAL RESULTS. COVERAGE OF SYMPTOMS IS DOWN TO 40%.

| Quantity | Cluster number | Symptom coverage (%) | Severity of symptoms |
|----------|----------------|----------------------|----------------------|
| 11 | 1~10 | 22~39 | 0.583140~0.761288 |

TABLE 4 EXPERIMENTAL RESULTS. COVERAGE OF SYMPTOMS IS DOWN TO 60%.

| Quantity | Cluster number | Symptom coverage (%) | Severity of symptoms |
|----------|----------------|----------------------|----------------------|
| 2 | 8~17 | 42~57 | 0.815955~0.895956 |

5. Conclusions

This study used thresholding, morphological operation and edge detection for pupil location, and applied 2-D Gabor filter to accurately showing feature region. The cluster

number and symptoms coverage is analyzed to output severity of symptom following fuzzy theory analysis, as shown in Tables 2, 3 and 4. In the future study, eigenvalue of iris texture will be classified by other classification methods, iris samples will be increased, as well as the examination of other organs.

References

- [1] Allie Simon and David M. Worthen, MD and Lt John A, "An Evaluation of Iridology", JAMA vol 242, No. 13, 1979.
- [2] J. Daugman, "High confidence visual recognition of persons by a test of statistical independence", IEEE Trans. Patt. Anal. and Machine Intell., vol.15, no.11, pp.1148-1161, 1993.
- [3] John Daugman, "How iris recognition works", IEEE Trans. on CSVT, vol.14, no.1, pp.21-30, 2004.
- [4] R.P. Wildes, "Automated, non-invasive iris recognition system and method", United States Patent, no.5572596, 1994.
- [5] Adhi Dharma Wibawa and Mauridhi Hery Purnomo, "Early Detection on the Condition of Pancreas Organ as the Cause of Diabetes Mellitus by Real Time Iris Image Processing", IEEE, 2006.
- [6] Lin Ma and Naimin Li, "Texture Feature Extraction and Classification for Iris Diagnosis", ICMB, LNCS 4901, pp.168-175, 2007.
- [7] R. A. Ramlee, S.Ranjit, "Using Iris Recognition Algorithm, Detecting Cholesterol Presence", IEEE, 2009.
- [8] Lotfi A. Zadeh, "Toward extended fuzzy logic—A first step", Fuzzy Sets and Systems 160 3175–3181, 2009.
- [9] Andrei Doncescu, Joseph Aguilar-Martin and Jean-Charles Atine, "Image color segmentation using the fuzzy tree algorithm T-LAMDA", Fuzzy Sets and Systems 158 230 – 238, 2007.
- [10] Isak Gath and Dan Hoory, "Fuzzy clustering of elliptic ring-shaped clusters", Pattern Recognition Letters 16 727-741, 1995.
- [11] R. S. Feris, T. E. Campos and R. M. C. Junior, "Detection and tracking of facial features in video sequences", in Mexican International Conference on Artificial Intelligence, pp. 129-137, 2000.
- [12] R. L. Hsu, M. A. Mottaleb, and A. K. Jain, "Face detection in color images", IEEE Trans. Pattern Analysis and Machine Intell., vol. 24, pp. 696-706, 2002.
- [13] O. R. Vincent and O. Folorunso, "A Descriptive Algorithm for Sobel Image Edge Detection", InSITE, 2009.